Ultimate strength characteristics of aluminium plates for high speed vessels

S. Benson, J. Downes & R.S. Dow
Newcastle University, UK

ABSTRACT:

Marine grade aluminium alloy has become an established structural material for medium to high speed commercial craft and has also been used as the primary hull material for several naval vessels including a 127 m trimaran. The analysis of large high speed craft operating in deep ocean and potentially hostile environments will require rigorous methodologies to evaluate the ultimate strength of the hull girder. This paper examines the strength of plate elements with a range of geometric, imperfection and material parameters typical of a high speed vessel using a non linear finite element approach. Representative plate load shortening curves are required in simplified hull girder ultimate strength methodologies; for the case of a high speed aluminium vessel the curves need to account for the effects of parameters including alloy type, imperfection, softening in the heat affected zone, residual stresses, lateral pressure and biaxial load. A parametric study presented in this paper shows that these factors have a significant influence on the strength behaviour of aluminium plates.

1 INTRODUCTION

Marine grade aluminium alloy has become an established structural material used for medium to high speed commercial craft operating in coastal locations throughout the world. The recent development of a 127 m aluminium Littoral Combat Ship (LCS) with a range of 4500 nm has shown the potential for aluminium to be a viable material for large, high speed, ocean going vessels. The advantages of aluminium alloys over steel for construction of such vessels include a high strength to weight ratio, good resistance to corrosion and comparable ease of manufacture. Future operational requirements for large high speed craft such as LCS will likely include exposed and potentially hostile deep sea environments for significant periods with the corresponding influence on strength requirements. The strength criteria for the hull will be primarily dependent on overall girder strength. Therefore the design of such vessels requires structural prediction techniques capable of producing a light structure with high confidence in its strength and safety.

The strength and stiffness of the deck and shell of a ship is governed by the strength of the individual plate and stiffener elements which together comprise the overall hull girder structure. The vessel strength depends critically on the behaviour of the plates under load combinations, particularly their instability characteristics in compression. The influence of local compressive failure on the ultimate strength of a hull is encapsulated in simplified methodologies to evaluate the ultimate longitudinal bending strength of the hull girder (Smith 1977). If such methodologies are to be adapted for large high speed craft, the compressive strength characteristics of aluminium plates typical of such vessels need to be assessed.

This paper examines the strength of plate elements with a range of geometric parameters typical of the midship scantlings of a high speed vessel. A parametric study examines the influence of geometric plate imperfections, material properties and internal stress fields using a non linear finite element method. The parameters are quantified using statistical information, rules and code specifications from various sources. Results from the study are compared to various design rules including Eurocode 9.

2 METHODS TO PREDICT COLLAPSE BEHAVIOUR OF ALUMINIUM PLATES

Empirical methods to predict the collapse strength of flat, rectangular, ship type plates take into account the departure from classical plate buckling theory due to the effects of imperfections, internal stresses and the additional post buckled strength of simply supported plates. Faulkner (1975) provides a history of the development of ultimate strength formulas for steel plate. Since this publication ultimate strength methods suitable for marine plating with various boundary conditions and loading scenarios have been further progressed.

For aluminium plating much of the recent research effort is encapsulated in various design codes, simplified formulae and computer programs used to calculate the ultimate collapse strength under in-plane and lateral load. Some commonly used methodologies for long plates in uniaxial compression are compared here along with several methods to predict the strength of biaxially loaded plates. This review is not exhaustive of the available methods, but gives an indication of the values likely to be used in design.

There are limited open source experimental test results for plates in uniaxial compression. A comprehensive physical test database of 5000 and 6000 series aluminium alloy plates under uniaxial compression was established at Cambridge University in the mid 1980s by Mofflin and Dwight (Collette 2005). The results of these tests provide a good basis for comparison of empirical methods.

2.1 *Uniaxial Compressive Load*

2.1.1 *Paik & Duran Regression Formula*

Paik & Duran (2004) developed a regression formula defining the ultimate strength of an unstiffened aluminium plate with a heat affected zone (HAZ). The formulation is based on finite element analysis of variously alloyed marine grade aluminium plates.

The effects of the HAZ are taken into account by defining an averaged slenderness ratio, taking into account the softened material alongside the longitudinal stiffener plate boundary:

$$\beta = \frac{b}{t}\sqrt{\frac{\sigma_{0eq}}{E}} \tag{1}$$

σ_{0eq} is an averaged material proof stress to take into account the reduced proof strength of the HAZ material, σ_{0HAZ}, over a specified breadth of plating away from the plate edge, b_{HAZ}. In the present study, the HAZ alongside the short edge boundary was found to have a negligible effect on plate strength behaviour and is therefore excluded from the calculation of the averaged proof stress. Therefore, the equation used here is a simplified form of the formulation proposed by Paik:

$$\sigma_{0eq} = \frac{(b-2b_{HAZ})\sigma_0 + 2b\sigma_{0HAZ}}{b} \tag{2}$$

where σ_0 is the 0.2% proof stress of the alloy.

2.2 *Faulkner Formula*

The Faulkner formula, as given in Equation 3, is possibly the most commonly used empirical method available in the marine industry to estimate the strength of simply supported steel plates under longitudinal compression (Guedes Soares 1988). The method has been found to correlate well with test data from various steel plate experiments (Faulkner 1975). The formula includes the effects of residual stress and distortion implicitly. Therefore the existence of a HAZ breadth should be ignored in the calculation of β.

$$\begin{aligned} \phi_x &= \frac{\sigma_{xav}}{\sigma_0} = 1.0 \qquad when\ \beta < 1 \\ \phi_x &= \frac{\sigma_{xav}}{\sigma_0} = \frac{2}{\beta} - \frac{1}{\beta^2} \quad when\ \beta \geq 1 \end{aligned} \tag{3}$$

A number of variations following the pattern of the Faulkner formula are also available, for example by the US DOD (1982) and by Wang et al. (2005). The latter reference is specific to aluminium and includes a correction to account for the softening in the HAZ.

2.2.1 *Eurocode 9*

Eurocode 9 (2007) is a detailed code specifying criteria in the design of structures made from wrought and cast aluminium alloys. The code includes an empirical formula for predicting ultimate plate strength in a similar form to Faulkner's method but with explicit corrections for the softening in the HAZ. The ultimate strength of a plate under uniform compression is given in the form of a limit state. For comparative purposes in this study the partial safety factors in the formulation are set to unity and, assuming a simply supported homogenous plate, the ultimate compressive force at collapse is defined in terms of an effective cross section area of the plate multiplied by the material proof stress. For the range of plates considered in this study the formulae to calculate the effective cross section can be written:

$$\begin{aligned} A_{eff} &= \min\begin{cases} 2b_{HAZ}t\rho_{0HAZ} + (b-2b_{HAZ})t\rho_c \\ bt\rho_c \end{cases} \\ \rho_c &= \frac{C_1}{\left(\beta/\varepsilon\right)} - \frac{C_2}{\left(\beta/\varepsilon\right)^2}\ ,\ \ \rho_{0HAZ} = \frac{\sigma_{0HAZ}}{\sigma_0} \end{aligned} \tag{4}$$

where β=b/t, rather than as defined in Equation 1 and $\varepsilon=(250/\sigma_0)^{0.5}$. The factors C_1 and C_2 depend on

the material classification; factors of 29 and 198 are specified for the marine grade alloys considered here.

2.2.2 *Comparison of Uniaxial Strength Methods*

Methods to predict uniaxial compression of long plates are compared in Figure 1 alongside relevant test data from the plate tests carried out by Mofflin (Collette 2005). Calculations are made for a typical 5083-H116 alloy plate of breadth 400mm, aspect ratio 3 and with a HAZ breadth of 25mm.

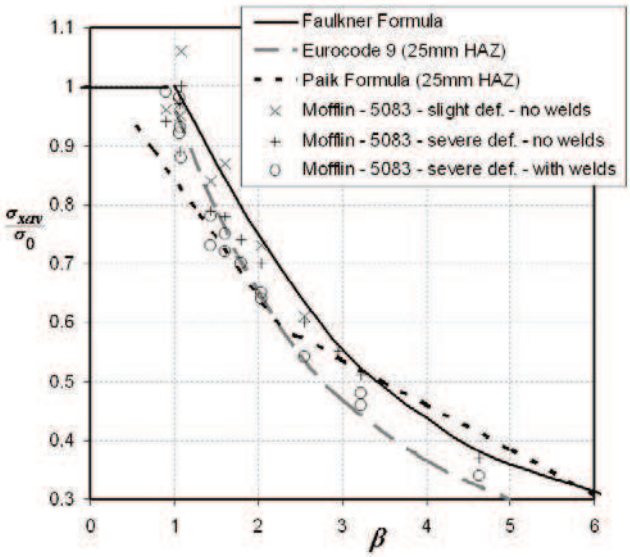

Figure 1. Comparison of methods to predict uniaxial plate strength

2.3 *Biaxial Load*

Plate strength under in-plane biaxial load is presented on interaction diagrams which compare the ultimate strength of the plate in the longitudinal and transverse directions. The applied longitudinal and transverse stresses are made non dimensional using the uniaxial compressive stress of the plate. Thus:

$$R_x = \frac{\sigma_{xav(MAX)}}{\sigma_{xav(yav=0,MAX)}} \qquad R_y = \frac{\sigma_{yav(MAX)}}{\sigma_{yav(xav=0,MAX)}} \tag{5}$$

Various formulae are presented in literature to predict the interaction of biaxial loads. The formulas generally take a similar form to the von Mises yield criterion with coefficients replacing the power terms (Paik & Thayamballi 2003) Neglecting the effects of edge shear and lateral pressure, the expression takes the form:

$$(R_x)^{c1} + \alpha R_x R_y + (R_y)^{c2} = 1 \tag{6}$$

This equation equates to the von Mises formula by setting *c1 = c2 = 2* and $\alpha = 1$, which is valid for plates in biaxial tension.

For biaxial compressive load, coefficients are given in a number of literature sources to predict the interaction curve (Paik & Thayamballi 2003). For example, Paik et al. (2001) suggests an adaptation of Equation 6, with *c1 = c2 = 2* and $\alpha = 0$ when both load components are compressive. DNV HSLC rules (2001) contains an interaction formula for aluminium plates which, for the slenderness ratios considered in this study, can be approximated to Equation 6 with the coefficients *c1 = 1, c2 = 1.2* and $\alpha = -0.8$.

A biaxial loading study specific to aluminium plates by Kristensen & Moan (1999), including the effects of HAZ and residual stress, found that the biaxial compressive interaction relationship is dependent on the slenderness ratio of the plate. A regression formulation defining the biaxial interaction as a function of slenderness is presented as follows:

$$R_x = \min\begin{cases} \dfrac{1-R_y^{\,2}}{1-(0.213-0.275(\beta-3))R_y} \\ 1+(0.05-0.1\beta)R_y \end{cases} \tag{7}$$

The calculation of β should assume a zero HAZ breadth as this is accounted for implicitly in the above regression equation. If β > 3, only the first formula in Equation 7 should be used.

A more detailed formulation is given by Kristensen (2001), taking into account the aspect ratio and slenderness of the plate to calculate coefficients for the interaction formula given in Equation 6. This was found to give similar results compared to Equation 7 and therefore the latter equation is used for comparative purposes in this paper. The biaxial relationships are compared in Figure 2 for a plate with slenderness ratio of 3.

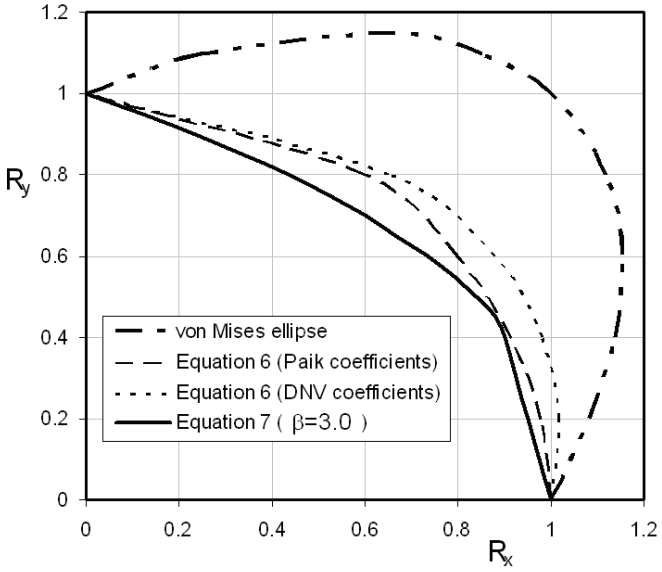

Figure 2. Comparison of methods to predict biaxial plate strength

3 CHARACTERISATION OF ALUMINIUM ALLOY PLATES

A welded ship structure will inevitably have geometric imperfections and residual stresses introduced

during construction and once the ship enters service. It is recognised that initial imperfections can have a significant effect on the ultimate strength of the plate (Ueda & Yao 1979). Therefore, a numerical model must be able to take into account any significant influence of geometric out of flatness, residual stresses and softening in the HAZ.

3.1 *Material Properties*

The strength characteristics of aluminium differ with steel in terms of its stress-strain relationship. Unlike steel, the curved non-linear region of the stress-strain relationship of aluminium does not exhibit a clear yield point. The ultimate elongation and ultimate strength to yield strength ratio is also lower than that of steel.

The grades of aluminium alloys typically used in the marine industry are the 5000 and 6000 series. A complete list of alloys certified for use in a marine environment is given by classification authorities including DNV and ABS, as summarised by Sielski (2007). However, the present study limits itself to investigating alloys 5083-H116 and 6082-T6, which are the most common alloys currently used by the marine industry.

Due to variations in the composition of the alloys the modulus of elasticity also varies, albeit modestly. In this study it is taken as 70GPa. Representative values of proof stress as defined by DNV are used in this study. A Ramberg-Osgood approximation is used to represent the stress strain curve in the analysis:

$$\varepsilon = \frac{\sigma}{E} + 0.002\left(\frac{\sigma}{\sigma_0}\right)^n \tag{8}$$

There is wide variation between different codes and literature sources to define the knee factor coefficient, n, and the 0.2% proof stress of the aluminium alloy. Representative coefficients based on a review of various sources are used here. Alloy 5083-H116 is specified with a 0.2% proof stress of 215MPa and a knee factor of 15. The 0.2% proof stress of alloy 6082-T6 is specified at 260MPa with a knee factor of 30.

Collette (2005) highlights the possibility that the proof stress of 5000 series alloys are often higher in tension than in compression due to the strain hardening method used in their production. Quoted values in this study, based on tensile coupon tests, do not take this phenomenon into account because no established test data has been found. This effect does need to be quantified to enable a more accurate material representation in future studies.

3.2 *Initial Geometric Imperfections*

Panels are subject to a highly inhomogeneous heat treatment during welding caused by the concentrated high temperature heat input of the weld tool. The effects of welding can be broadly separated into three categories, as the process: changes the material properties in the HAZ; causes distortion of the plating due to local straining; and creates a residual stress field.

Welding induced distortion can include transverse and longitudinal shrinkage of the plate close to the weld, angular rotation of the plating around the weld bead axis, longitudinal bending of the plate-stiffener combination, rotational distortion and buckling distortion. In practice, angular change (wrap up) and longitudinal bending have been found to be the significant contributors to weld induced plate distortion (Paik & Thayamballi 2003). Misalignment and forcing together of panel elements will also result in initial out of straightness and imperfections may be further exacerbated during vessel operations.

3.2.1 *Geometric Imperfection Amplitude*

Localised distortions have been found to vary significantly for plates with different slenderness ratios, with slender plates exhibiting much larger local imperfections (Smith et al. 1988).

Numerous surveys have been carried out to measure the geometric imperfections in welded plating, with most focusing on steel plated structures. Empirical formulae to define the maximum initial imperfection amplitude, w_{opl} usually assume the imperfection magnitude is either proportional to β or to β^2 (Paik & Thayamballi 2003). Measurements of the deflection amplitude in bottom plating of a British Naval frigate in 1965 and reported by Faulkner (1975) shows closer dependence on β^2.

A well known formulation is proposed by Smith et al. (1988). Statistics of the imperfections in box girder bridges and shell plating of ships are drawn together and equations for slight (3% percentile), average and severe (97% percentile) imperfections in steel plate are derived as follows:

$$\frac{w_{opl}}{t} = \begin{cases} 0.025\beta^2 & \text{for slight level} \\ 0.1\beta^2 & \text{for average level} \\ 0.3\beta^2 & \text{for severe level} \end{cases} \tag{9}$$

Very similar imperfection criteria are derived from an extensive study of aluminium plates recently carried out for the Ship Structure Committee (Paik et al. 2008). A more simplified alternative formulation is given by Paik & Duran (2004) based on limited data from numerous sources including Zha & Moan (2001):

$$w_{opl} = 0.009b \tag{10}$$

Representative deflection amplitude according to Equation 10 is used in this study and compared with the amplitude as given by Equation 9.

3.2.2 *Geometric Imperfection Shape*

Imperfection of a rectangular steel plate is idealised as a single half wave shape along the plate length with localised distortions superimposed and a single half wave shape in the short direction.

The elastic buckling mode of a simply supported plate under uniaxial compression normally forms an approximate pattern of square sinusoidal half waves (Smith et al. 1988). However, inelastic buckling and collapse nucleates into a localised buckle with a wave length less than or equal to the aspect ratio a/b. It is well recognised that the shape of the initial deflection can significantly affect the formation of these collapse mode shapes in a uniaxially loaded plate.

Previous studies have shown that the plate collapse mode is strongly influenced by the initial deflection shape. For example, a study by Masaoka & Mansour (2004) shows snap through buckling in a uniaxially compressed plate as the deflection mode changes from the initial deflection mode to the preferred buckling mode. Certain initial imperfection shapes may even increase plate strength by stopping formation of the preferred buckling mode (Smith et al. 1988).

A Fourier series imperfection shape is typically used to define plate imperfection, where the deflection amplitude w_0 at any point on the plate surface is defined as a function of the maximum deflection, w_{opl}.

$$w_0 = w_{opl} \sum_{i=1}^{M} B_i \sin\frac{i\pi x}{a} \sin\frac{\pi y}{b} \qquad (11)$$

The initial distortion coefficients, B_i, represent the influence of each mode shape contributing to the overall imperfection shape. All other terms are as shown in Figure 3.

A combination of multiple mode shapes using the Fourier series can represent a measured plate imperfection shape, but the choice of representative coefficients depends on a high number of varying factors that contribute to an assumed overall imperfection shape. A typical representation combining a single half wave and a square half wave imperfection with the ratio 0.8/0.2 is often used. A number of different Fourier representations are compared in the parametric study presented in this paper.

However, a study by Dow & Smith (1984) assessing the effects of localised imperfections due to dents compared to half wave type imperfections along the entire plate length concluded that representing this form of imperfection as a Fourier series is unsatisfactory. The study found that a square wave Fourier component shape may give a non conservative representation of the imperfection if localised distortion is present. This effect is noted, although it is not considered in the present study.

3.3 *Material Softening in the HAZ*

The welding process causes a strength reduction in the heat affected material adjacent to the weld. The formation of HAZ is due to different metallurgical processes for the 5000 and 6000 series alloys. 5000 series alloys are work hardened in the milling process. Subsequently, the high heat of fusion welding raises the temperature of material that is close to the weld above the re-crystallisation temperature, removing the work hardening and leaving the material in the weaker annealed state. In 6000 series alloy, the heat generated during welding causes the magnesium silicide precipitates, which provide extra strength in the alloy, to turn back into solution in the weld itself. Further away from the weld the precipitates grow in size, which reduces the local alloy strength.

3.3.1 *HAZ Material Properties*

Because the local transient temperature during welding decreases with increased distance from the weld, the material properties in the HAZ region also change with distance from the weld. However, for the purposes of numerical analysis, the HAZ is usually idealised to have constant reduced material properties over a defined width of plating away from the weld centre line location.

Material properties in the HAZ are determined by mechanical testing, although several inconsistencies between experiments, including the length of the test specimen and the method of forming the coupon, means that data from different sources has wide variation (Sielski 2007). In this study an idealised HAZ block with a strength knock down factor of 0.67 for 5083-H116 and 0.53 for 6082-T6 has been selected based on DNV guidance (2001).

3.3.2 *HAZ Breadth*

The HAZ breadth can be established by testing the hardness of the area close to the boundaries of welded plates. Hardness tests are reported by Zha & Moan (2001) and Paik (2004). Both these papers propose a 25mm HAZ breadth, originally proposed as a “1-inch rule” by Mazzolani (1995).

Zha & Moan use representative HAZ breadths of 12.5mm and 25mm in numerical analyses of plates. These HAZ breadths are repeated by Collette (2005) in analysis of box sections. Paik uses a HAZ breadth of 3 times the plate thickness, consistent with DNV guidance (2001).

BS8118 (1991) and Eurocode 9 (2007) give explicit formulae to estimate the HAZ breadth. The formulas give HAZ breadth as a function of the plate/stiffener thickness. However, for the range of

plate slenderness' considered in this study the codes give HAZ breadths similar to the 1 inch rule. Therefore, a representative HAZ breadth of 25mm is used in the parametric study presented here.

3.4 *Residual Stress*

Residual stress is the term used to describe self equilibrated internal stresses present in otherwise unstressed structural elements. They arise when some or all areas of a structural member undergoes physical or thermal induced deformation and is subsequently prevented from returning to its previous non deformed state. This creates a permanent, inhomogeneous deformation field in the structural member. It is well known that residual stress fields are generated in most metal structures and manufactured parts during construction (Stephens et al. 2001).

For welded aluminium panels the most significant cause of residual stress is the welding process itself (Sielski 2007). The residual stress field develops from the formation of a continuous weld. The liquid weld bead is resisted from contracting as it cools by the bulk of the parent material. This causes tensile residual stresses to be created within and near to the weld and corresponding balanced compressive stresses in material away from the HAZ.

The intensity of the heat input from welding is a function of a number of variables, including: the type of weld procedure used; the pass size; and the depth of penetration (Mazzolani 1995). Recent studies have found that the heat input and associated mechanical properties of the material at high temperatures is the significant contributor to residual stresses for both molten state (arc) and solid state (friction stir) welding (Peel et al. 2003; Withers 2007). This suggests that the quantity of heat introduced during welding is the primary contributor to residual stress rather than the specific levels of plastic deformation caused by the weld method.

For the purposes of numerical analysis, the welding induced residual stress field can be idealised into stress blocks, as depicted in Figure 3. A relationship between the residual stress and the width of the tensile stress field is:

$$b_t = \frac{\sigma_{rcx}}{2\left(\sigma_{rcx} - \sigma_{rtx}\right)} b \tag{12}$$

An empirical approach to estimate the compressive residual stress of steel plates is given by Smith et al. (1988):

$$\frac{\sigma_{rcx}}{\sigma_0} = \frac{\sigma_{rcy}}{\sigma_0} = \begin{cases} -0.05 \text{ for slight level} \\ -0.15 \text{ for average level} \\ -0.3 \text{ for severe level} \end{cases} \tag{13}$$

However, measurements in a recent Ship Structure Committee experiment programme indicate tensile residual stresses well below the parent metal strength and closer to the assumed HAZ strength (Paik et al. 2008). As an example, using representative values for b_t of 25mm for a 400mm plate in Equation 12 and 13 gives a predicted tensile stress well in excess of the assumed HAZ proof strength as defined previously, suggesting that the differences of aluminium compared to steel, including heat conduction rate and the HAZ softening, means that Smith's approach may not be valid for use.

Based on these findings, a tensile residual stress equal to the HAZ proof stress in a block of equal width to the HAZ breadth is used in the parametric analyses conducted in this study. Compressive residual stresses are calculated to give a self equilibrated resultant stress as given by Equation 12.

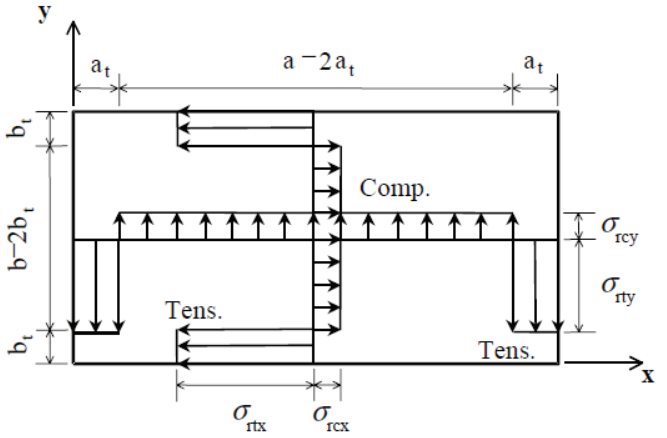

Figure 3. Idealised residual stress distribution with weld along all four edges of the plate (Paik & Thayamballi 2003).

4 FINITE ELEMENT METHODOLOGY

Abaqus finite element analysis software was used to carry out the parametric study. The Abaqus solver has geometric and material non linear capabilities and has been shown to provide good comparative results to test data of plates in compressive instability (Zha & Moan 2001).

An incremental arc length analysis utilising the Riks method copes with negative slopes on the iteration curve which are typical of plate collapse analyses when the plate loses strength in the post collapse region. The incremental form of the analysis enables production of complete load shortening curves in the post processing module.

Quadrilateral shell elements with reduced integration were used for all plates modelled in the parametric study. A check on result convergence for different mesh densities was carried out and based on these results the mesh for all plates was specified so that at least one element, and more usually two, spans the HAZ region. Element type and mesh size are consistent with previous studies (Zha & Moan 2001).

Initial imperfection is introduced by applying an out of plane Fourier series displacement to each

node using an external subroutine to directly edit the node input file. Residual stress is introduced using the *INITIAL CONDITIONS feature of Abaqus, which allows elements to be prescribed an initial stress field prior to any displacement of the model.

The plate is modelled to represent support on all sides by longitudinal stiffeners at the long edges and transverse frames at the short edges. The supports are assumed to be relatively stiff along the boundary, preventing out of plane deformation and constraining the edges to remain straight throughout the analysis. The plating is assumed to be continuous across several frame and stiffener spans and therefore the stiffeners are assumed to provide no rotational restraint about the edge axis, resulting in a simply supported boundary condition at all edges.

Load is applied with a displacement control on one edge perpendicular to the load direction. This ensures edges remain straight throughout the application of load. Unloaded edges are free to move in-plane but are constrained to remain straight.

In the biaxial compression analyses a fixed load is applied on the long edges as an initial load step prior to an incremental compressive displacement applied on the short edges. The long edges remain free to move in-plane, allowing the biaxial transverse force to remain constant throughout the longitudinal compressive displacement load step.

5 COLLAPSE BEHAVIOUR OF ALUMINIUM PLATES IN UNIAXIAL COMPRESSION

This section presents a parametric study which assesses the influence of geometric and material factors characterising aluminium ship plating in uniaxial compression. A series of load shortening curves, calculated using the finite element method, compare the influence of plate slenderness, aspect ratio, fabrication related distortion, material softening in the HAZ and the residual stress field.

Load shortening curves are presented in non dimensional form. The applied force on the loaded plate edge is used to calculate an average applied stress, σ_{xav}, assuming that the cross section area of the plate remains constant throughout the analysis. The applied stress is then divided by the welded plate proof stress. Similarly, the displacement of the loaded edge is divided by the unloaded plate length to give the strain and then further divided by the coupon strain, ε_0, at 0.2% proof stress to give results in non dimensional form.

5.1 *Effects of Aspect Ratio, Slenderness and Alloy*

Load shortening curves are presented in Figures 4 and 5 for various plates with slenderness ratio between 1.5 and 5.0 in uniaxial compression. Levels of imperfection and residual stress are modelled using the rules and assumptions described previously in this paper, consisting of: an imperfection magnitude of 4mm; an imperfection shape superimposing 80% single half wave and 20% square half wave distortion; a 25mm HAZ with reduced strength material; a residual tension field equal to the softened material proof stress; and a self equilibrating residual compression field. The results for plates modelled with a residual stress field in the x-direction only are presented; initial analyses found minimal differences between equivalent plates with a biaxial residual stress field. For the same reasons results for plates with the HAZ modelled in the long edges only are given here, consistent with initial findings and in previous studies (Zunaidi 2007).

5.1.1 *Aspect Ratio*

Analyses of three different thickness plates modelled with aspect ratios between 1 and 4 are compared in Figure 4. The results show similar characteristics before and after collapse, although the peak strength at collapse varies slightly. The initial imperfection shape of the square plate is equivalent to the nucleated collapse shape, causing the load shortening curve to depart immediately from a linear elastic response.

A typical longitudinal framed midship of a high speed vessel will likely be made up of long plates predominantly loaded in the longitudinal direction. Therefore the load shortening behaviour of plates with higher aspect ratios are more relevant to this study and an aspect ratio of 3 is therefore further studied here.

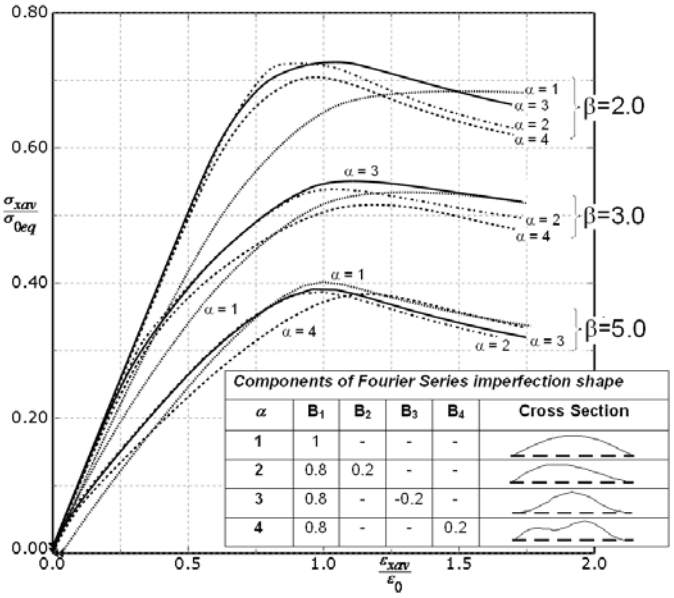

Figure 4. Load shortening curves for typical 5083 plates with average imperfections and residual stresses.

5.1.2 *Slenderness Ratio*

In keeping with the simplified formulae based methods described previously, a progressive decrease in overall plate strength occurs as the slenderness ratio increases, as shown in Figure 5. The shape of the

load shortening curves initially follows a similar pattern for all slenderness ratios and for both alloy types, following the linear elastic stress-strain relationship of the material. This indicates an initial phase of load shortening predominantly due to in-plane compression of the plate.

The load shortening curves for slender plates make a deviation from the linear elastic relationship well before collapse. This is characterised by a transition from the initially imposed imperfection to a shape equivalent to the buckling mode. The plate then exhibits stable behaviour as it continues to withstand further increases in load. Through this phase the central area of the plate increasingly deflects out of plane, escaping the applied load and causing an increasing portion to be taken by the side regions. Eventually the plate undergoes elasto-plastic deformation with a resulting loss of load carrying capacity.

The deviation point from the initial phase is less distinct for more stocky plates where elastic buckling stresses are approximately equal to or greater than the overall collapse strength. This is particularly apparent for low slenderness 6082 plates. In these cases the transition from the linear region to collapse is relatively rapid.

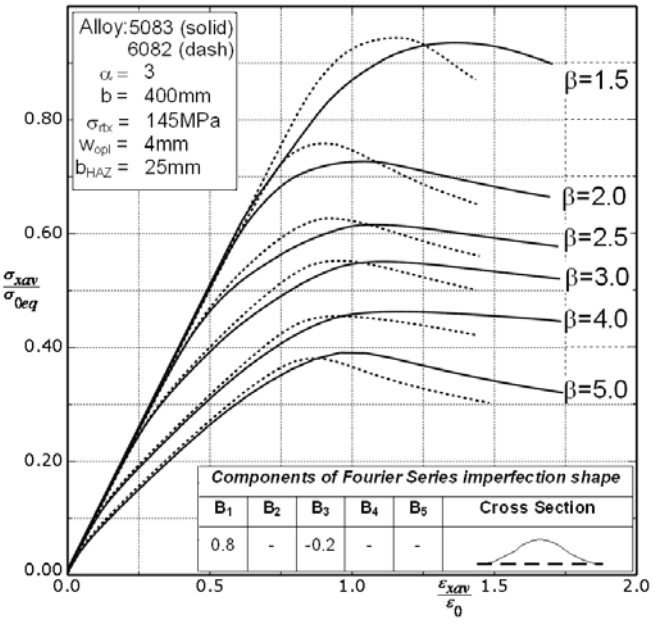

Figure 5. Load shortening curves for typical 5083 and 6082 plates with average imperfections and residual stresses.

5.1.3 *Alloy Type*

Comparing both alloys in Figure 5 shows differences in the pre and post collapse regions of the load shortening curve. These resemble the corresponding differences in the alloys stress strain curve, where 5083 has a more rounded transition away from the elastic region compared to 6082. The 6082 alloy appears to provide slightly higher ultimate strength for the lower β values and lower ultimate strength for the higher slenderness plates. In all cases the 6082 plates exhibit more rapid load shortening in the post collapse region.

5.2 *Effects of Imperfection Shape and Amplitude*

A series of imperfection models have been analysed to demonstrate the variability of the plate behaviour in the pre and post collapse phases during the application of uniaxial compression. Figure 6 presents a sample of the results for two plates with slenderness ratio of 2.0 and 3.0. A comparison of results for both plates demonstrate significant differences in the load shortening curve in the pre collapse region, suggesting that the initial imperfection shape has significant influence on the strain response in this region. Clearly this will be of importance in a progressive collapse analysis including plate elements.

For the more stocky plate shown in Figure 6 the imperfection shape also has a significant effect on the overall collapse strength. This is less apparent for the more slender plate, despite the significant differences in the shortening curve before the collapse load is reached.

The effects of imperfection amplitude have been tested by comparing Equation 10 given by Paik with the average and severe imperfection magnitudes as given by Smith in Equation 9. For the range of plates tested here the average imperfection given by both equations are similar, particularly for the more stocky plates. This results in very similar load shortening curves in Figure 7. Use of the severe deflection amplitude equation causes a reduction in the overall collapse strength of the plate. In all cases, the load shortening curve maintains the same overall shape regardless of imperfection magnitude, with only the peak position affected.

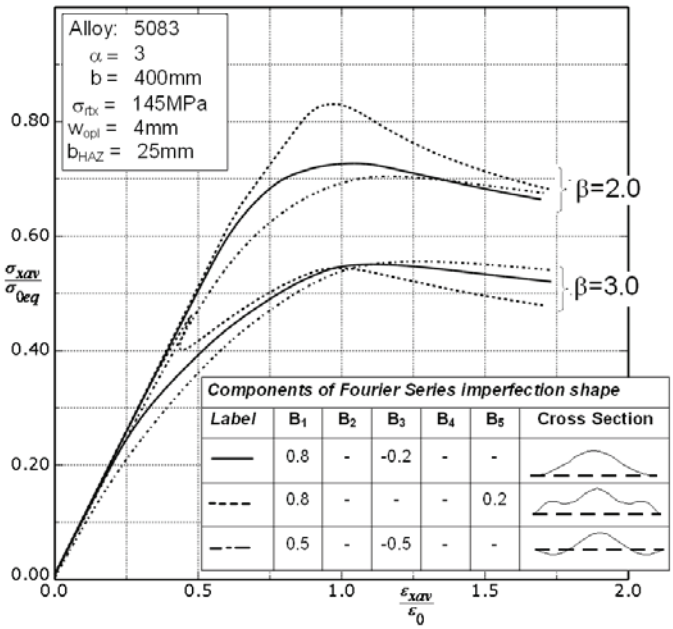

Figure 6. Load shortening curves for typical plates with different initial imperfection shapes.

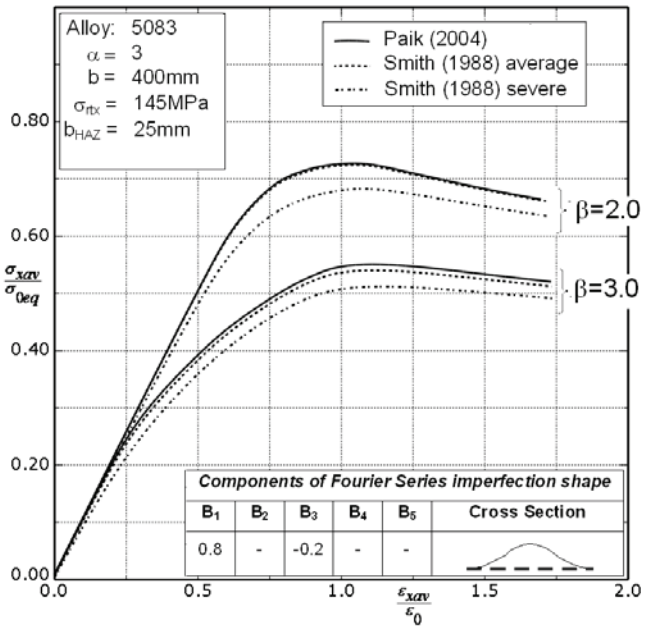

Figure 7. Load shortening curves for typical plates with different initial imperfection magnitude.

5.3 *Effects of HAZ*

Representative HAZ breadths of 12.5mm, 25mm and 50mm are compared in Figure 8 for β = 2.0 and 3.0. For each model the residual stress distribution was adjusted to match the HAZ breadth. The plots show that HAZ breadth has a significant influence on the collapse strength of the plate, primarily by shifting the transition away from the initial linear elastic phase. From this point onwards the shape of the load shortening curve remains unaffected by the size of the HAZ breadth.

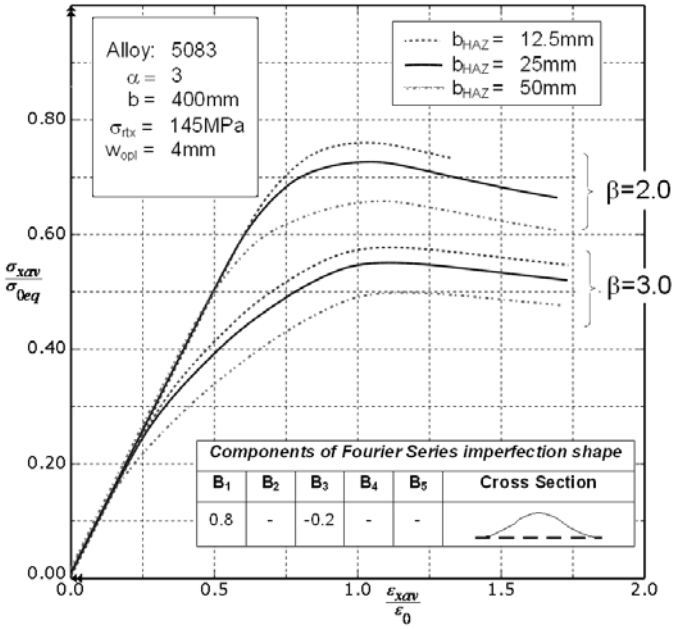

Figure 8. Load shortening curves for typical plates with different HAZ breadth and typical geometric distortions

5.4 *Effects of Residual Stress*

A plate with a residual stress field as proposed previously is compared to a plate with zero residual stress in Figure 9. Comparisons are made for a full range of plate slenderness. For all except the most stocky plate analysed here, the results indicate that the residual stress has a moderate impact on the plate collapse characteristics. For intermediate slender plates the zero residual stress case diverges from the residual stress case in the pre collapse region, resulting in higher magnitude collapse strength. The very slender plate (β=5) also shows different characteristics after the collapse load has been passed.

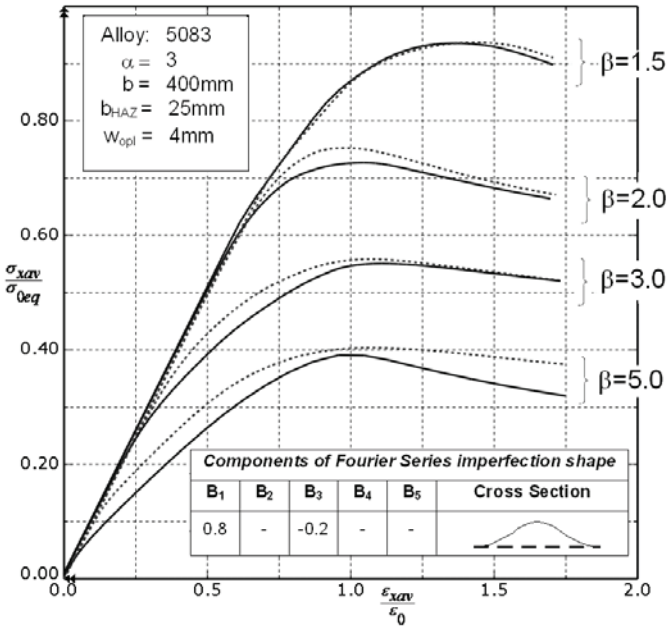

Figure 9. Load shortening curves for typical plates with residual stress field (full) and without residual stress field (dashed).

5.5 *Effects of Lateral Load*

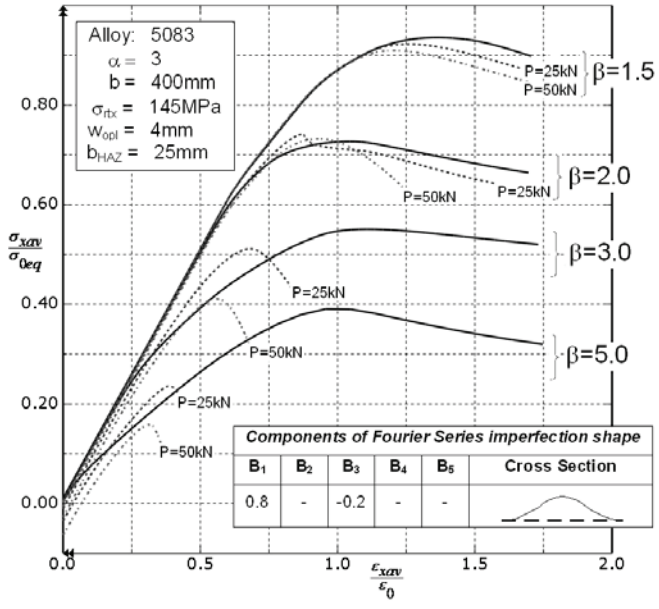

Figure 10. Comparison of typical plates with lateral load of 25kN and 50kN applied on the concave side of the plate

Limited analyses were undertaken for plates in uniaxial compression with a fixed lateral load, P, applied uniformly across the plate surface. The load is assumed to act on the concave side of the distorted plate, exacerbating the imperfection amplitude. The

load is equivalent to a hydrostatic pressure on the side or bottom shell of the vessel. Pressure loads of 25kPa and 50kPa, equivalent to a hydrostatic pressure depth of approximately 2.5m and 5.0m respectively, are compared in Figure 10. The results demonstrate an increasingly adverse effect of lateral pressure as the slenderness of the plate increases.

5.6 *Comparison with Empirical Results*

Plate collapse strength values for a limited selection of analyses from Sections 1.1 to 1.4 are compared with the Eurocode 9 formula in Figure 11. The results for the average imperfection levels, as described previously in Section 5.1, show reasonable correlation with the shape of the Eurocode 9 curve, although predicted strength here is higher in all cases, suggesting a slight conservatism in the code formula. The influence of the imperfection and HAZ parameters tested in this study has a moderate effect on the ultimate strength value, with the most pronounced differences occurring in the intermediate slenderness region of Figure 11.

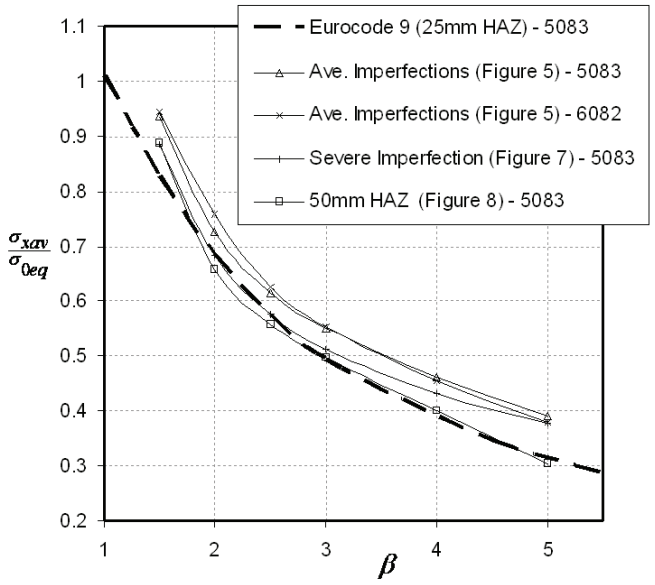

Figure 11.Ultimate strength of typical plates as a function of slenderness ratio. Comparison with Eurocode 9 formulation.

6 COLLAPSE BEHAVIOUR OF ALUMINIUM PLATES IN BIAXIAL COMPRESSION

This section presents a limited analysis set of 5083 alloy plates in biaxial compression. It is intended that the analyses presented here will be expanded in a future paper to investigate different material and residual stress representations along with the influence of further load combinations.

Interaction curves for plates with slenderness ratios between 1.5 and 4.0 are given in Figure 12. A HAZ breadth of 25mm is assumed at all 4 edges along with a biaxial residual stress distribution as in Figure 3 with tensile stresses equal to the HAZ proof stress and balanced compressive stresses calculated using Equation 12. The results are presented as non dimensional functions of the parent material 0.2% proof stress, rather than the equivalent proof stress used in previous sections.

The curves show an initial region from the x axis where the collapse strength is relatively unaffected by the increasing biaxial load on the long edges. This region is more pronounced for the lower slenderness plates, and becomes less distinct as the slenderness increases.

The analysis results are compared with the closed form method of Kristensen & Moan (Equ. 7) and with the von Mises type interaction formula (Equ. 6) using the coefficients as given by Paik. To enable direct comparison with the analysis results the empirical formulations, which calculate non dimensional values R_x and R_y, are further multiplied by the non-dimensional uniaxial strength of the plate loaded in the corresponding direction as calculated in this study.

The results from this study show good correlation to the closed form Kristensen equation for all slenderness ratios analysed, demonstrating the effect of slenderness on the behaviour of a plate under biaxial load. The simple expression as given by the von Mises type formula cannot be adjusted to take into account the slenderness of the plate, unless specific formulations for the coefficients are specified, as is done by Kristensen (2001).

It is clear from these results that a biaxial load combination has a varying effect on the strength of aluminium panel elements depending on the slenderness of the plate. The results suggest that further studies of the effects of biaxial load are required to identify the load shortening curve paths for use in ultimate strength methodologies of stiffened panels and hull girder structures under biaxial bending.

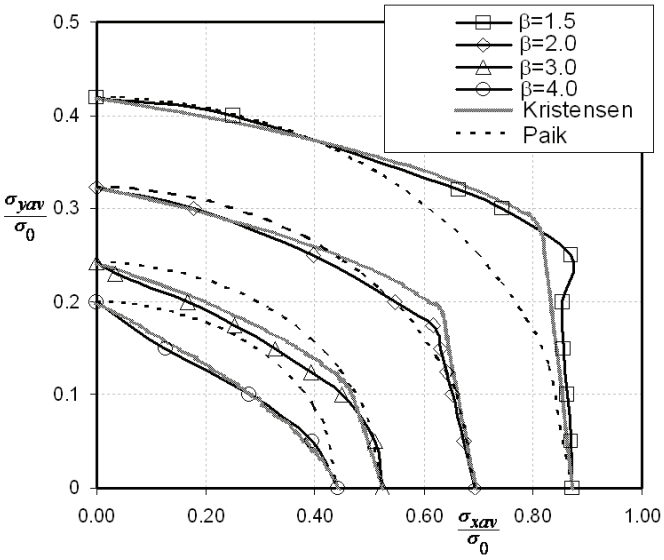

Figure 12. Ultimate strength of typical 5083 alloy plates in biaxial compression. Imperfection shape as given in Figure 5.

7 CONCLUSIONS

The imperfection of ship type aluminium plates are defined by a number of parameters which together describe the geometric imperfection, material properties, softening in the HAZ and the residual stress field. Code formulations such as Eurocode 9 explicitly take into account many of the parameters examined in this study and provide a good correlation to the ultimate strength of plates modelled in uniaxial compression using non linear FEA.

Representative plate load shortening curves are required in simplified hull girder ultimate strength methodologies; for the case of a high speed aluminium vessel the curves need to account for the effects of alloy type, imperfection, softening in the heat affected zone and residual stress. This study has shown that the parameters have a significant influence on the strength behaviour of aluminium plates in uniaxial compression both before and after the collapse load is reached. The effects of lateral pressure and biaxial loading also have a significant effect on the collapse strength and load shortening curve of the plates. An ultimate collapse method specific to a large high speed aluminium hull girder will need to adequately account for these parameters.

ACKNOWLEDGEMENTS

This present study was undertaken with the support of the Office of Naval Research. The first author would also like to thank Mr John Garside for his insightful discussions on the subject of this study.

REFERENCES

British Standards 1991. *Structural Use of Aluminium.* BS8118:Part 2.

British Standards 2007. *Eurocode 9: Design of aluminium structures.* BS EN 1999-1-1:2007.

Collette, M. 2005. *The strength and reliability of aluminium stiffened panels.* PhD Thesis. School of Marine Science and Technology, Newcastle University.

Naval Sea Systems Command. 1982. Design Data Sheet 100-4 - Strength of Structural Members.

DNV. 2001. *Rules for Classification of High Speed, Light Craft and Naval Surface Craft.* Det Norske Veritas.

Dow, R. S. & Smith, C. S. 1984. Effects of Localized Imperfections on Compressive Strength of Long Rectangular Plates. *Journal of Constructional Steel Research* 4: 51-76.

Faulkner, D. 1975. A review of effective plating for use in the analysis of stiffened plating in bending and compression. *Journal of Ship Research* 19(1): 1-17.

Guedes Soares, C. 1988. Design Equation for the Compressive Strength of Unstiffened Plate Elements with Initial Imperfections. *Journal of Constructional Steel Research* 9: 287-310.

Kristensen, O. H. H. & Moan, T. 1999. Ultimate Strength of Aluminium Plates under Biaxial Loading. *FAST 1999*.

Kristensen, O. H. H. 2001. *Ultimate Capacity of Aluminium Plates under Multiple Loads, Considering HAZ Properties.* Dr. Ing Thesis. Department of Marine Structures, Norwegian University of Science and Technology, Trondheim.

Masaoka, K. & Mansour, A. 2004. Ultimate Compressive Strength of Imperfect Unstiffened Plates: Simple Design Equations. *Journal of Ship Research* 48(3): 191-201.

Mazzolani, F. M. 1995. *Aluminium alloy structures*. London: E & FN Spon.

Paik, J. K. & Duran A. 2004. Ultimate Strength of Aluminum Plates and Stiffened Panels for Marine Applications. *Marine Technology* 41(3): 108-121.

Paik, J. K. & Thayamballi A. K. 2003. *Ultimate limit state design of steel-plated structures*. Wiley.

Paik, J. K., Thayamballi, A. K. et al. 2001. Advanced Ultimate Strength Formulations for Ship Plating Under Combined Biaxial Compression/Tension, Edge Shear, and Lateral Pressure Loads. *Marine Technology* 38(1).

Paik, J. K., Thayamballi, A. K. et al. 2008. *Mechanical Collapse Testing on Aluminum Stiffened Panels for Marine Applications*. Ship Structure Committee.

Peel, M., Steuwer, A. et al. 2003. Microstructure, mechanical properties and residual stresses as a function of welding speed in aluminium AA5083 friction stir welds. *Acta Materialia* 51: 4791-4801.

Sielski, R. A. 2007. *Aluminum Marine Structure Design and Fabrication Guide*. Ship Structure Committee.

Smith, C. S. 1977. Influence of local compressive failure on ultimate longitudinal strength of a ship's hull. *PRADS 1977*: 73-79.

Smith, C. S., Davidson, P. C. et al. 1988. Strength and Stiffness of Ships' Plating under In-plane Compression and Tension. *Transactions of the Royal Institution of Naval Architects.* 130: 277-296.

Stephens, R. Fatemi, A. et al. 2001. *Metal fatigue in engineering.* Wiley-Interscience.

Ueda, Y. & Yao T. 1979. Ultimate Strength of a Rectangular Plate under Thrust : with Consideration of the Effects of Initial Imperfections due to Welding. *Transactions of Japanese Welding Research Institute*. 8(2): 257-264.

Wang, X., Sun, H. et al. 2005. Buckling and Ultimate Strength of Aluminium Plates and Stiffened Panels in Marine Structures. *Fifth International Forum on Aluminium Ships*. Tokyo, Japan.

Withers, P. J. 2007. Residual stress and its role in failure. *Reports on Progress in Physics* 70: 2211-2264.

Zha, Y. & Moan T. 2001. Ultimate strength of stiffened aluminium panels with predominantly torsional failure modes. *Thin Walled Structures* 39: 631-648.

Zunaidi, A. N. 2007. *The Strength Characteristics of Aluminium Panels in Ships.* MSc Thesis. School of Marine Science and Technology, Newcastle University.